A&A manuscript no.
(will be inserted by hand later)

Your thesaurus codes are:
02. (11.17.1; 12.12.1)

ASTRONOMY AND ASTROPHYSICS
May 8, 2000

Space-time distributions of QSO absorption systems

A.D. Kaminker*, **A.I. Ryabinkov**, **D.A. Varshalovich**

A.F. Ioffe Physical Technical Institute, Politekhnicheskaya 26, 194021 St.-Petersburg, Russia

Received xx August 1999 / Accepted ...

Abstract. A statistical analysis of the distributions of C IV and Mg II absorption-line systems observed in quasar spectra within the cosmological redshift interval $z = 0.2 - 3.2$ is presented. The results indicate that the overall z-distribution of absorbing matter is non-uniform: it has statistically significant maxima and minima, but it appears statistically isotropic. The maxima in the z-distribution of absorption systems are found at $z_m = 0.44, 0.77, 1.04$, 1.30, 1.46, 1.60, 1.78, 1.98, 2.14, 2.45, 2.64, and 2.86 (± 0.04). The positions of maxima and minima of the z-distribution turn out to be the same (within the statistical uncertainty) for different celestial hemispheres independently of their orientation. The resulting space-time distribution of absorbing matter resembles successively embedded spheres corresponding to the z_m values indicated. The most probable origin of such a distribution is an alternation of pronounced and depressed epochs in the course of cosmological evolution.

Key words: galaxies: quasars: absorption lines – cosmology: large-scale structure of Universe

1. Introduction

Most cosmological models are based on the cosmological principle (e.g., Peebles 1993) which assumes that all points of space and all directions of observations are equivalent, so that the Universe is, on average, uniform and isotropic. It was reliably confirmed by the latest observations of Cosmic Microwave Background at the relative level $\lesssim 10^{-5}$ at least up to arc-degree scales. On the other hand, the local distribution of matter surrounding our Galaxy is not uniform. Moreover, there exists a hierarchy of scales of galaxy clusters and superclusters in addition to familiar small-scale inhomogeneities of galaxies (e.g., Bahcall 1995). The largest known inhomogeneities of matter form the so–called Large-Scale Structure (LSS) discovered in the last decade at moderate redshifts ($z \lesssim 0.6$) (e.g., Broadhurst et al. 1990, Landy et al. 1996, Einasto et al. 1997). It is quite probable that the specific scale of the largest inhomogeneities has changed noticeably in the course of the cosmological evolution. Therefore it is worth while to investigate the uniformity and isotropy of the distribution of matter on larger cosmological space-time scales at higher redshifts. In particular, one can use available observational data on redshifted absorption-line systems imprinted on spectra of quasars (QSOs) for a statistical analysis of absorbing material at redshifts $z \gtrsim 1$.

The analysis of some line-of-sight spatial correlation function for C IV absorption-line systems in QSO spectra was carried out by Quashnock et al. (1996) in the redshift interval $z = 1.2 - 4.5$. They found the clustering of C IV absorbers on comoving scales comparable with the LSS (see Sect. 4). However, the correlation function they used could not represent completely general properties of the z-distribution of the absorbing matter.

The degree of uniformity and isotropy of the distribution of C IV absorption systems at $z = 1.2-3.2$ was analyzed by Ryabinkov et al. (1998) . Here we present results of an investigation of the distribution of absorption matter in a wider redshift interval $z = 0.2-3.2$. We use the absorption lines of the resonance doublets C IV ($\lambda_1^0 = 1548$ Å and $\lambda_2^0 = 1551$ Å), and Mg II ($\lambda_1^0 = 2796$ Å and $\lambda_2^0 = 2804$ Å) as indicators of absorbing material existing at the redshifts under study (subscripts 1 and 2 numerate

Send offprint requests to: A.D. Kaminker
* E-mail: kam@astro.ioffe.rssi.ru

lines of doublets, superscript 0 denotes laboratory values). These spectral lines are usually observed in QSO spectra with high emission-line redshift z_e. We assume that the redshift of the absorption lines z_a is cosmological , i.e., $\lambda = \lambda^0(1+z_a)$, and the observed absorption-line systems are associated with ionized gas in intervening galaxies or clusters of galaxies at large cosmological distances along the line-of-sight between QSO and observer.

Notice that an analysis of the z-distribution of photon mean free paths based on the statistics of QSO absorption-line systems has been performed recently by Liu & Hu (1998). Using the data on QSO absorption redshifts from the catalog of Junkkarinen et al. (1991) they found that the mean free path displays quasi-periodic component with alternating sharp maxima and minima in addition to the monotonic trend. We will show that these results appear to be qualitatively consistent with the results presented here, although our observational data and statistical approach are rather different.

In Sect. 2 we present statistical evidence for a non-uniform — sequence of significant maxima and minima — but an isotropic distribution of matter using data on C IV and Mg II absorption systems in the redshift intervals $z = 1.2-3.2$ and $z = 0.2-2.1$, respectively. Similar results obtained by the analysis of the normalized distribution which enable us to avoid some of observational selection effects are given in Sect. 3. In Sect. 4 we discuss some effects of possible clustering of the absorbing matter on the set of maxima and minima revealed. In Sect. 5 we present tests of possible regularity of the distribution obtained. Conclusions and possible consequences of the results are discussed in Sect. 6 .

2. Analysis of C IV and Mg II absorption systems

2.1. Criteria of sampling

We consider inhomogeneous statistical material since we use available data on QSO spectra obtained in different studies, which applied different criteria for line detection and system identification. In such a situation, probabilities of registration of absorption systems could be *a priori* different for different values of z, and this could simulate non-uniformity of z-distributions. Additional selection effects may be induced by the non-cosmological movement of absorbing matter in the nearest neighborhood of QSOs and by small-scale clustering of close absorption features corresponding to clouds within one galaxy. In order to reduce an influence of all such selection effects one should analyse available data using a unified procedure of sampling.

Let us start from the determination of criteria and conditions which are used in our discussion. We consider the wavelength intervals in the observed QSO spectra between emission lines C IV and Ly-α as well as Mg II and Ly-α. The boundaries of these intervals are determined in terms of their redshifts $z^i_{\rm min} \le z_a \le z^i_{\rm max}$, where the index $i = 1, 2, ..$ covers all observations of the QSO spectra sampled for the analysis. The values $z^i_{\rm min}$ and $z^i_{\rm max}$ are set to obey additional conditions:

$$\begin{aligned} z^i_{\rm min} &\ge \frac{1.5R_i}{\lambda^0_2 - \lambda^0_1} - 1; \\ z^i_{\rm max} &\le z_e - \frac{v_e}{c}\,(1+z_e), \end{aligned} \qquad (1)$$

where R_i = FWHM$_i$ represents the spectral resolution (in Å) for the i-th spectral interval, and v_e = 3000 km/s is the velocity shift allowed for the absorption system relative to the corresponding emission line. The first condition rejects all unreliable doublets and the second one eliminates absorption systems with an essential part of their redshifts due to non-cosmological origin, e.g., expansion of QSO envelopes. Thus, only absorbers (intervening galaxies or clusters of galaxies) situated quite far from the corresponding QSOs were sampled for our consideration. In this way we selected $N_{\rm QSO} = 398$ of observed spectral intervals for 250 QSOs.

For each i-th spectral interval we calculate the threshold value of the absorption equivalent width

$$W^i_{\rm th} = \frac{5}{1+z^i_{\rm min}}\,\frac{R_i}{< S/N >_i}, \qquad (2)$$

where $< S/N >_i$ is the signal-to-noise ratio averaged over the whole i-th interval. An absorption line with an equivalent width in the rest frame $W_\lambda/(1+z_a) \ge W^i_{\rm th}$ could have been reliably detected in the i-th interval of the redshifts. We adopt also the equivalent width of the weaker line (λ^0_2) of a doublet as the equivalent width of the absorption system $W_{\rm abs}$.

In order to reveal possible large scales and suppress small scales, we take into account only separate absorbers eliminating the well-known tendency of the neighboring absorption systems to cluster on a velocity scale $\Delta v \lesssim 600$ km/s (see, e.g., Val'tts 1991, Steidel & Sargent 1992, Quashnock et al.

1996). Therefore, we consider any two close systems z'_a and z''_a situated along the line of sight as a single one with $z_a = (z'_a + z''_a)/2$ and $W_{\rm abs} = W'_{\rm abs} + W''_{\rm abs}$ under the condition

$$\frac{\Delta v}{c} = \frac{\Delta z}{1+z_a} \leq 0.002, \tag{3}$$

where c is the speed of light, and $\Delta z = |z'_a - z''_a|$.

To make the statistics of selected absorption systems more homogeneous we use two criteria of sampling of observational data: *detection* and *identification*. Let us assume that $n_i \geq 0$ absorption systems of C IV or Mg II were registered with redshifts z_a^{ij} and equivalent widths in the rest frame $W_{\rm abs}^{ij}$, in each i-th spectral interval, where index $j = 1, 2, ...n_i$, for $n_i \geq 1$, numerates all observed systems inside the i-th interval. Then the criterion of the *detection* of j-th absorption system is

$$W_{\rm abs}^{ij} = \left(\frac{W_{\rm abs}}{1+z_a}\right)^{ij} \geq W_{\rm th}^{i}, \tag{4}$$

where $W_{\rm th}^i$ is determined by Eq. (2).

The criterion of *identification* for the resonance doublets of C IV or Mg II consists of two conditions:

$$\left|\frac{\lambda_2}{\lambda_2^0} - \frac{\lambda_1}{\lambda_1^0}\right| \leq 10^{-3};$$
$$1 \leq \frac{W_{\lambda 1}}{W_{\lambda 2}} \leq 2, \tag{5}$$

where $W_{\lambda 1}$ and $W_{\lambda 2}$ are the equivalent widths of doublet lines with account of their uncertainties.

2.2. Uniformity of the distributions

According to the criteria described in Sect. 2.1 we considered 299 C IV absorption systems in the redshift interval $z = 1.2-3.2$ and 216 Mg II absorption systems in the interval $z = 0.2 - 2.1$, observed in QSO spectra (Bergeron et al. 1987; Boisse & Bergeron 1985; Caulet 1989; Foltz et al. 1986; Khare et al. 1989; Lanzetta et al. 1987; Lanzetta & Bowen 1992; Petitjean & Bergeron 1990; Robertson et al. 1986, 1988; Sargent et al. 1982, 1988a, 1988b, 1989, 1990; Sargent & Steidel 1987; Steidel 1990; Steidel & Sargent 1992; Turnshek et al. 1989; Young et al. 1982).

Our starting hypothesis (null-hypothesis) is the assumption of uniform distributions of the samples relative to linear functions (trends) $N_{tr} = a + bz$, obtained in the redshift intervals $z = 1.2 - 3.2$ and $z = 0.2 - 2.1$ for C IV and Mg II systems and subtracted in the following analysis. We divide these intervals into n equal independent bins and determine the trends by the Least Squares Method. Let us note, that for the data separated for our analysis, we obtain insignificantly weak trends.

According to the null-hypothesis, probabilities p_k of an absorption system to fall into various bins numerated by k $(k = 1, 2, ..., n)$ are the same and equal to $p_k = 1/n$. To estimate the empirical probabilities p_k we determine the n frequency values $\omega_k = N_{\rm k}/N_{\rm abs}$, where $N_{\rm k}$ is the number of systems falling in the k-th bin and $N_{\rm abs}$ is the full number of absorption systems considered ($N_{\rm abs} = \sum_{k=1}^{n} N_{\rm k}$). The set of frequencies ω_k represents the set of random values which can be approximately associated at $\sqrt{N_{\rm k}} > 3$ with Gauss distributions with mean values $\bar{\omega}_k = p_k$ and mean-square deviations $\sigma_k(\omega_k) = \sqrt{\bar{\omega}_k(1-\bar{\omega}_k)/N_{\rm abs}}$, which are mutually dependent. It is more convenient, however, to use transformed random quantities

$$\tilde{\omega}_k = \int_0^{\omega_k} \frac{{\rm d}\omega'_k}{\sigma_k(\omega'_k)} = 2\sqrt{N_{\rm abs}}\,{\rm arcsin}(\sqrt{\omega_k}) \tag{6}$$

also described by Gauss distributions but with the unified dispersions equal to $\tilde{\sigma}_k = 1$. Let us calculate the quantities

$$X^2 = \sum_{k=1}^{n} (\tilde{\omega}_k - \bar{\tilde{\omega}})^2 = \sum_{k=1}^{n} \left[(\tilde{\omega}_k)^2 - (\bar{\tilde{\omega}})^2\right], \tag{7}$$

where $\bar{\tilde{\omega}} = (\sum_{k=1}^{n} \tilde{\omega}_k)/n$. The quantity X^2 in Eq. (7) is distributed as χ^2 with $(n-1)$ degrees of freedom (dof). When $X^2 > \chi^2_{1-p}$, where χ^2_{1-p} is the tabulated value of χ^2 corresponding to a given significance level p, the hypothesis that the absorption systems are uniformly distributed can be rejected with a confidence $\beta = 1 - p$.

Figs. 1a and b represent the calculated values of X^2 as functions of the number of bins n into which the intervals of z are divided. Fig. 1a refers to C IV absorption systems in the redshift interval $z = 1.2 - 3.2$. Comparison of the calculated X^2 and tabulated χ^2_{1-p} values allows us to reject the hypothesis that the distribution is uniform for $n \geq 6$ with confidence $\beta = 0.998$ (3σ level). The absorption-system distributions appear to be non-monotonic for $n \geq 6$, and have local maxima (peaks) and minima (depressions) relative to the trends of the distributions (see Figs. 2 and 3). As follows from Fig. 1a, an excess of the calculated X^2 over the tabulated χ^2_{1-p} values in the case of C IV systems is most appreciable when the number of bins is $n = 9$ and 28. This indicates that

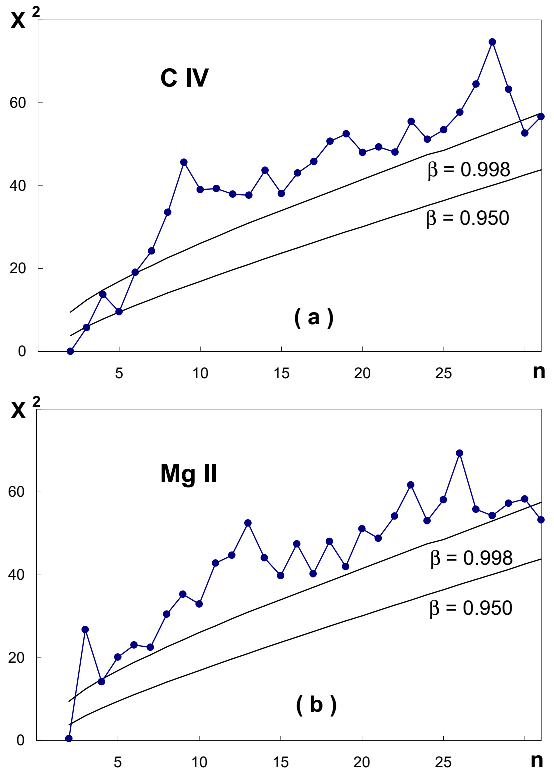

Fig. 1. Comparison of X^2 values calculated using Eq. (7) and tabulated values χ^2_{1-p} plotted for two confidence levels $\beta = 1 - p = 0.998$ (upper smooth line) and $\beta = 0.950$ (lower smooth line) for dividing of the entire redshift interval into n bins: (a) C IV systems in the redshift interval $z = 1.2 - 3.2$, (b) Mg II systems in the redshift interval $z = 0.2 - 2.1$.

the deviation from uniform z-distribution is most pronounced when the total redshift interval is divided into these numbers of bins. The z distribution for $n = 9$ has two broad peaks, which divides into eight narrower peaks if n is increased. We chose $n = 28$ for the z-distribution of C IV systems, corresponding to the bin width $\Delta z = 0.071$. Fig. 1b refers to Mg II systems in the redshift interval $z = 0.2 - 2.1(2.057)$. In this case the excess of the calculated X^2 over the tabulated values χ^2_{1-p} is most noticeable when the number n of bins is 3, 13, 23, 26. We chose $n = 26$ which corresponds to the same width of bins, $\Delta z = 0.071$, as in the case of C IV systems.

Let us note, that at $n > 28$ for C IV and $n > 26$ for Mg II systems additional peaks appear in the z-distributions due to statistical fluctuations. However, such additional peaks turn out to be statistically insignificant ($< \sigma$) and we will not consider them further.

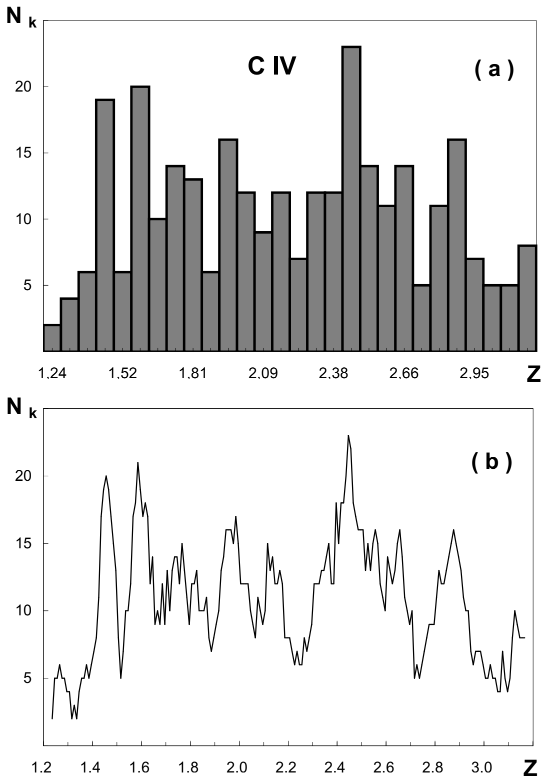

Fig. 2. z-distribution of 299 absorption systems of C IV : (a) histogram with bin size $\Delta z = 0.071$, (b) sliding-average distribution with averaging bin 0.071 and step 0.01 (see text for details).

Figs. 2a and b show the z-distribution of the 299 C IV absorption systems at $n = 28$. Fig. 2a is a histogram obtained for independent bins with $\Delta z = 0.071$. The peak positions in Fig. 2a depend on the first point of the histogram chosen arbitrary. In order to eliminate such an arbitrariness we represent in Fig. 2b the distribution obtained in so-called sliding-average approach, in which a set of consecutive shifts is performed of an averaging bin $\Delta z = 0.071$ along the z-axis with a step 0.01.

We determine the positions of the maxima (peaks) z_m as weighted mean values (centers of gravity) of the points forming a peak relative to the trend of the distribution obtained in the sliding-average approach. The corresponding values of z_m are 1.46, 1.60, 1.78, 1.98, 2.14, 2.45, 2.64, and 2.86, with accuracy ± 0.04 (half of the bin width). The significance levels of the peaks are estimated as $3\sigma, 3\sigma, \sigma, 2\sigma, \sigma, 3\sigma, 2\sigma$, and 2σ, respectively.

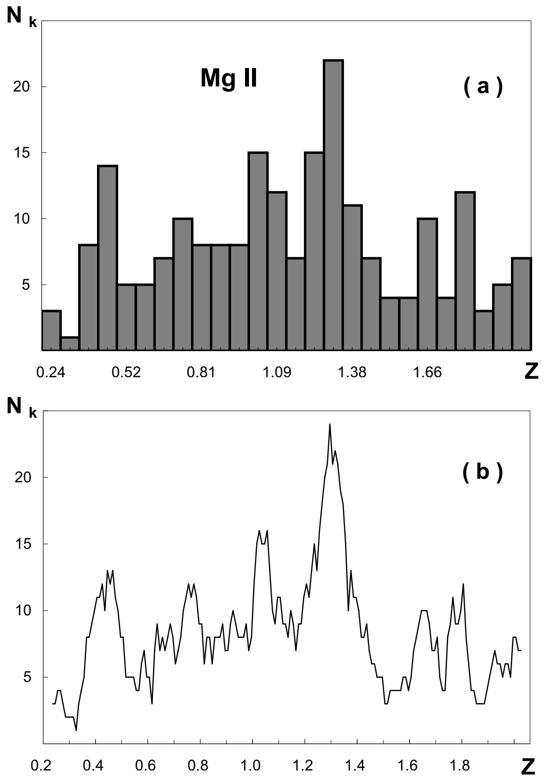

Fig. 3. Same as Fig. 2, but for 216 absorption systems of Mg II.

The results for Mg II absorption-line systems are quite consistent with the results discussed above. Figs. 3a and b show the z distribution of 216 Mg II absorption systems for $n = 26$. Fig. 3a is the histogram obtained for independent bins with the same width $\Delta z = 0.071$ as in Fig. 2a. Fig. 3b shows the distribution obtained in the sliding-average approach. The values of the centers of gravity of the peaks are equal $z_m = 0.44$, 0.77, 1.04, 1.30, 1.66, and 1.78 (± 0.04). The significance values of the peaks are $2\sigma, \sigma, 3\sigma, 4\sigma, \sigma$, and σ, respectively. One can see, that the last two peaks of Mg II systems are in a good agreement with the second and third peaks in the distribution of C IV systems. However, the first conspicuous peak at $z_m = 1.46$ in the z-distribution of C IV systems is not seen in Fig. 3.

Thus, our results concerning both C IV and Mg II absorption systems provide evidence for non-uniform distribution of matter in the redshift interval $z = 0.2 - 3.2$ at a confidence level higher than 0.998.

2.3. Isotropy of the distributions

We test isotropy (or anisotropy) of distributions by comparing the z-distributions of C IV and (separately) Mg II systems in opposite independent hemispheres. For this purpose we divide the celestial sphere (Equatorial coordinates) into two hemispheres separated by the plane passing through the world axis ($\delta = \pm 90°$, δ is a declination) and rotate this plane about the world axis by steps $\Delta\alpha = 15°(1^h)$, where α is a right ascension. In such a way we obtain 12 pairs of independent hemispheres. For each hemisphere, we obtain the z-distribution of the absorption systems, the linear trends (see Sect. 2.2) having been excluded in all hemispheres. Let us note that dividing the celestial sphere into smaller parts leads to an increase of statistical errors. We calculate the correlation coefficient r for each pair of independent hemispheres and compare it with tabulated values r_β of the sample correlation coefficient for a given sample size n and the confidence level β (dof= $n - 2$).

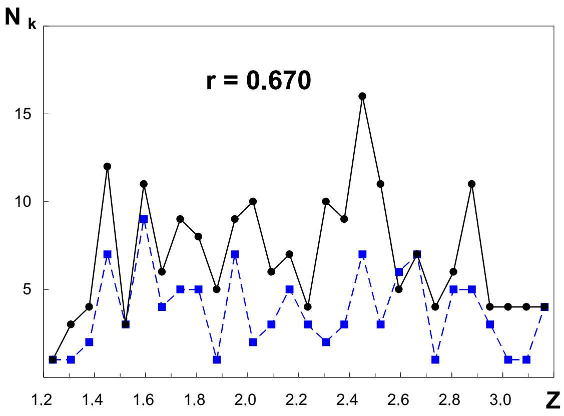

Fig. 4. z-distributions of C IV absorption systems in two opposite hemispheres $\alpha = 0 - 180°$ (filled circles) and $\alpha' = 180 - 360°$ (filled squares). The correlation coefficient r is indicated.

Fig. 4 shows the z-distributions in two opposite hemispheres $\alpha = 0 - 180°$ and $\alpha' = 180 - 360°$. The calculated correlation coefficient for these two distributions is $r = 0.670$, while $r_\beta = 0.588$ for $n = 28$ and $\beta = 0.999$; this provides evidence that the two distributions obtained are correlated better than at the 3σ level.

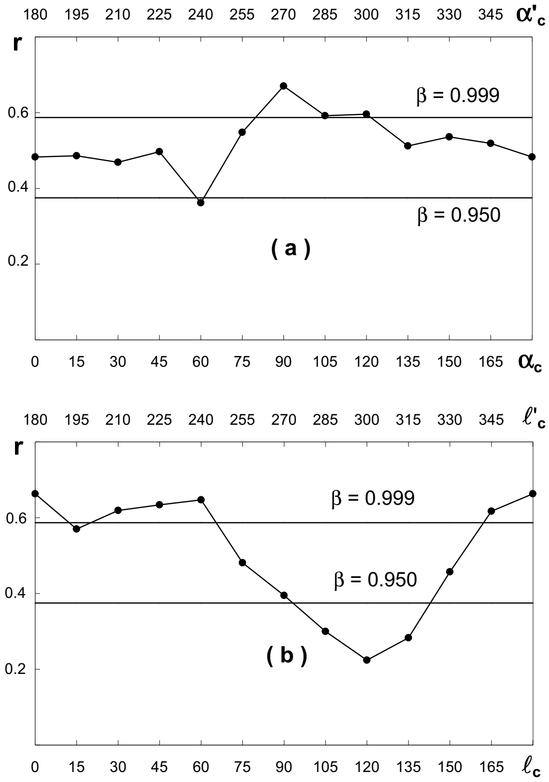

Fig. 5. Correlation coefficient r for the z-distributions of the C IV absorption systems in pairs of opposite hemispheres for Equatorial and Galactic coordinate systems: (a) dependence r on the right ascensions α_c (bottom horizontal axis) and α'_c (top horizontal axis) of the centers of two complementary hemispheres, (b) dependence r on the Galactic longitudes l_c (bottom horizontal axis) and l'_c (top horizontal axis) of the centers of two complementary hemispheres. The tabulated values $r_\beta = 0.588$ for the confidence level $\beta = 0.999$ ($> 3\sigma$) and $r_\beta = 0.375$ for $\beta = 0.950$ (2σ) are represented.

Fig. 5a represents the correlation coefficients for the z-distributions in pairs of opposite hemispheres as a function of the right ascensions of the centers of the hemispheres for two complementary intervals $0 \le \alpha_c \le 180°$ (lower horizontal axis) and $180° \le \alpha'_c \le 360°$ (upper horizontal axis). It is clear that the correlation of the z-distributions is significant, as a rule, at the 2σ level ($\beta \ge 0.95$). To verify that the positions of the distribution maxima do not depend on an orientation of the rotation axis we also performed the procedure described

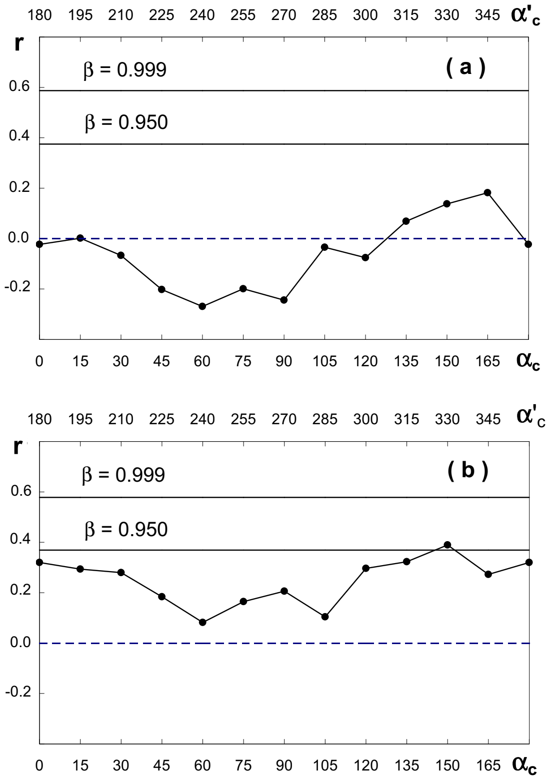

Fig. 6. Same as Fig. 5a, but for simulations of an isotropic distribution of 312 independent random numbers within C IV redshift interval $1.2 - 3.2$ (see text for details): (a) typical realization for a few hundred trials; (b) peculiar (rare) realization with $r > r_\beta$ for $\beta = 0.950$. Horizontal dash lines denote zero level of correlation.

above but with another rotation axis. We use the Galactic coordinates (l, b) (l and b are the Galactic longitude and latitude) instead of the Equatorial ones, and rotate a plain dividing the sky on two hemispheres about the axis passing through the North and South Galactic poles. Fig. 5b represents the correlation coefficients for the z-distributions as a function of the Galactic longitudes of the centers of the hemispheres for two complementary intervals $0 \le l_c \le 180°$ (lower horizontal axis) and $180° \le l'_c \le 360°$ (upper horizontal axis). One can see that the significance level of the correlation exceeds 2σ in most directions.

Low confidence levels for the correlation coefficients between pairs of hemispheres corresponding to the longitude intervals $105° \le l_c \le 135°$ and $285° \le l'_c \le 315°$ are associated with an apparent lack of observational data in the interval of the Galactic longitudes $280° \lesssim l \lesssim 320°$ (see Paper I).

In the case of Mg II systems the correlation on the 2σ level occurs in only half of the 12 pairs of opposite hemispheres due to insufficient statistics.

For comparison with the results plotted in Fig. 5a we produced a few hundreds of numerical simulations of an isotropic distribution of 312 independent random points within the interval of values $(1.2 - 3.2)$, which corresponds to the available statistics of C IV absorption systems. To imitate the isotropic distribution of absorption systems over the celestial sphere we produce 13×24 matrices for each numerical realization, where 24 consecutive sets of random numbers correspond with different celestial sectors ($\Delta\alpha = 15°$). Boundaries between the sets (neighbor columns of the matrices) are marked by values $\alpha_c = 0°, 15°, 30°, \ldots$ To simulate a z-distribution for the hemisphere with definite α_c we use $13 \times 12 = 156$ random points in 12 consecutive columns around the value α_c. In this way we calculate the correlation coefficients between the distributions obtained in pairs of opposite hemispheres (in our simulations).

Fig. 6a shows the correlation coefficient versus α_c for a typical realization. One can see that in most cases the values of $r(\alpha_c)$ are noticeably lower than the value $r_\beta = 0.375$ for $\beta = 0.95$ (2σ confidence level). $4 - 5$ peculiar realizations were found per hundred trials with values r reaching the confidence level $\beta = 0.95$ for a restricted interval of "α_c". One such peculiar realization is plotted in Fig. 6b. It essentially differs from the values $r(\alpha_c)$ plotted in Fig. 5a, where r exceeded the confidence level $\beta = 0.95$ for all values of α_c except one. In all numerical simulations we have failed to get $r(\alpha_c)$ similar to the dependence represented in Fig. 5a.

Figs. 7 and 8 show sets of the redshift distributions of the C IV and Mg II systems for the 24 hemispheres (the step of rotations is 15°). They may be treated as two-dimensional distributions: the vertical axes in Figs. 7a and 8a correspond to the right ascension of the hemisphere centers α_c in degrees, the horizontal axes correspond to redshift z. The light domains display an enhanced number of the absorption systems per redshift bin (number density), and the dark domains display reduced number densities. 9 gradations of grey color were used between white for maximum and black for minimum of the number density. Black domains are those for which we do not have necessary data. In Fig. 7a one can see continuous vertical light bands for C IV systems with centers at the same values of z_m as found in Sect. 2.2, i.e., $z_m = 1.46, 1.60, 1.78, 1.98, 2.45,$ and 2.86. Put another way these values z_m are independent of α_c within statistical uncertainty. The light bands at $z_m = 2.14$ and 2.64 are seen to be more fragmentary, probably due to lack of statistics. Similar results (but of lower statistical significance) follow from Fig. 8a for Mg II systems. One can notice at least four conspicuous vertical light bands with the centers at $z_m = 0.44$, 1.04, 1.30, 1.66, (see Sect. 2.2), and a few more fragmentary bands.

The vertical axes in Figs. 7b and 8b correspond to the Galactic longitude l_c (in degrees) of the hemisphere centers. It is clear from comparison of Figs. 7a and b, and Figs. 8a and b, that the positions of the vertical light bands as well as their widths do not change (within the errors) if one uses Galactic coordinates. Consequently, they do not depend on a direction (orientation of a hemisphere) in which the observations were accumulated. Let us note that the break noticeable in all light bands near Galactic longitude $l_c = 300°$ in Fig. 7b, and the less definite one in Fig. 8b, is likely to be associated with absence of observational data mentioned above. Qualitatively two-dimensional distributions of C IV and Mg II systems are consistent within the statistical uncertainties.

Thus our results on C IV and Mg II absorption-line systems may be treated as evidence for: (i) existence of statistically significant maxima and minima in the z-distribution of the systems at certain z-values, and (ii) independence of the values z_m of hemisphere orientations (hence of directions on the celestial sphere). The first point was noted by other authors, whereas the second one (as far as we know) was not mentioned previously (see Sect. 6).

3. Normalized distributions of absorption systems

In spite of the sampling criteria described in Sect. 2.1 the statistical material considered in Sect. 2 remains inhomogeneous. In order to minimize observational selection effects one can obtain so called normalized z-distributions of the absorption systems that ensure *a priori* equal probabilities for the detection and identification of the absorption systems. We use some modification of the usual approach of normalized distributions described, e.g., by Wolfe et al. (1986), Lanzetta et al. (1987), Steidel & Sargent (1992). Let us introduce the minimum rest equivalent width $W_{\min}$ and so called "redshift path density" or number

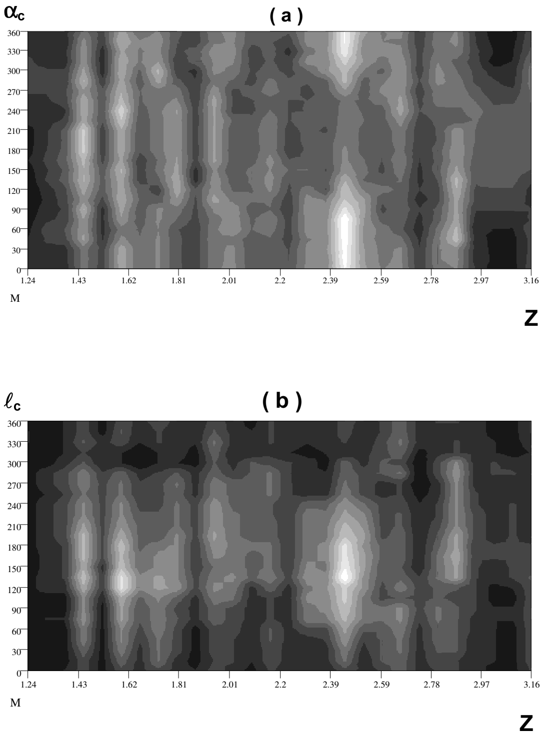

Fig. 7. z-distributions of C IV absorption systems in 24 hemispheres in the Equatorial and Galactic coordinates shown as light and dark regions of z (horizontal axis): (a) hemispheres are determined by the right ascensions $\alpha_c - 90° \leq \alpha \leq \alpha_c + 90°$, and the declinations $-90° \leq \delta \leq +90°$, the vertical axis corresponds to α_c in degrees; (b) hemispheres are determined by the Galactic longitude $l_c - 90° \leq l \leq l_c + 90°$, and the latitude $-90° \leq b \leq +90°$, the vertical axis corresponds to l_c in degrees.

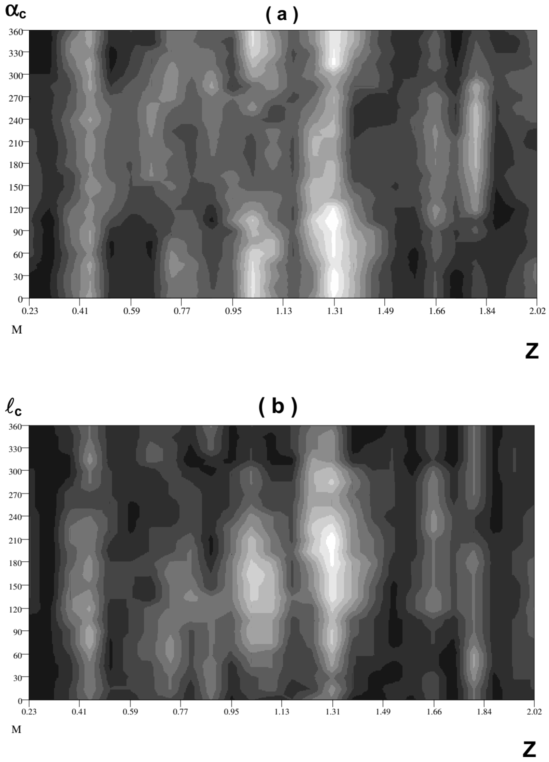

Fig. 8. Same as Fig. 7, but for Mg II absorption systems.

of observed QSO spectral intervals $(\Delta N_{\rm QSO})_k$ in which C IV or Mg II absorption systems with the equivalent width $W_{\rm abs}/(1+z_a) \geq W_{\rm min}$ (see Sect. 2.1) could have been registered at redshift z inside k-th redshift interval (bin) $z_k - z_{k-1} = \Delta z$ (see Sect. 2.2)

$$
\begin{aligned}
(\Delta N_{\rm QSO})_k & \\
&= \sum_{i=1}^{N_{\rm QSO}} H(z_{k-1} - z^i_{\rm min}) \\
&\times\ H(z^i_{\rm max} - z_k) H(W_{\rm min} - W^i_{\rm th}), \qquad (8)
\end{aligned}
$$

where $H(x)$ is the Heaviside step function. The quantity $(\Delta N_{\rm QSO})_k$ includes both spectra of sufficiently high quality ($W_{\rm th} \leq W_{\rm min}$), in which absorption systems were really detected ($n_i \geq 1$), and those, in which they were not ($n_i = 0$). We determine also the number of absorption systems $(\Delta N_{\rm abs})_k$ actually observed in the same k-th redshift interval

$$
\begin{aligned}
(\Delta N{\rm abs})_k & \\
&= \sum_{i=1}^{N_{\rm QSO}} H(z_{k-1} - z^i_{\rm min}) H(z^i_{\rm max} - z_k) \\
&\times\ H(W_{\rm min} - W^i_{\rm th})\, H(n_i - 1) \\
&\times\ \left[\sum_{j=1}^{n_i} H(z_k - z^{ij}_a) H(z^{ij}_a - z_{k-1}) \right. \\
&\times\ \left. H(W^{ij}_{\rm abs} - W_{\rm min}) \right]. \qquad (9)
\end{aligned}
$$

The normalized redshift distribution per unit redshift interval is the ratio of Eq. (9) to Eq. (8) and to the interval Δz

$$
\left(\frac{{\rm d}N}{{\rm d}z} \right)_k = \frac{(\Delta N{\rm abs})_k}{(\Delta N_{\rm QSO})_k \Delta z}. \qquad (10)
$$

The ratio $\Delta N\text{abs}/\Delta N_{\text{QSO}}$ characterizes the probability of registration of absorption systems in a given interval Δz in all possible observations of the proper quality, $W_{th} \leq W_{\min}$. As a result of preliminary analysis, we choose some optimal value of $W_{\min} = 0.2$ Å. Additional selection of QSO spectra and absorption-line systems associated with Eq. (10) reduces the amount of observational material to be included in the statistical analysis by factors of about 2 and 4 for C IV and Mg II systems, respectively. However, in addition to the statistical analysis described in Sect. 2, it is useful to perform similar analysis using the normalized z-distributions which are not subject to observational selection effects.

3.1. Uniformity of the normalized distributions

As in the case described in Sect. 2.2 we calculate linear trends, $\overline{(\mathrm{d}N/\mathrm{d}z)}_{\text{tr}} = a + bz$, in the redshift interval $z = 1.2 - 3.2$ using the Least Squares Method. For C IV absorption systems we obtain a noticeable trend: $a = 0.26 \pm 0.06$ and $b = -0.06 \pm 0.03$. After subtraction of the trend we can check the hypothesis of uniform distributions using the χ^2 method (see Sect. 2.2). It was confirmed at a significance level of 2σ that the distribution of absorbing material (with elimination of the trend) is non-uniform and has local maxima and minima.

Fig. 9 shows the normalized z-distribution (probability of registration) of the C IV absorption systems for $n = 28$ and $W_{\min} = 0.2$ Åat $\Delta z = 0.071$. The positions of the maxima (centers of gravity) of the peaks $z_m = 1.45$, 1.63, 1.78, 1.95, 2.11, 2.38, 2.63, and 2.91, with accuracy ± 0.04 are in agreement with the positions of z_m determined in Sect. 2.2. Estimates of significance levels for the peaks should be produced, taking into account the quantity ΔN_{QSO} and the ratio in Eq. (10). As a result we have $2\sigma, 2\sigma, \sigma, 2\sigma, 2\sigma, 2\sigma, 2\sigma$, and σ, respectively, estimated relative to the trend.

In the case of Mg II systems only 51 absorption doublets satisfy Eq. (9). It makes results of the analysis for the normalized distribution of Mg II still much less statistically significant than the results obtained for C IV systems. Nevertheless, such an analysis yields qualitative confirmation for the main conclusion of Sect. 2. Thus we obtain strongly non-uniform z-distribution of Mg II systems with alternating maxima and minima similar to those obtained for C IV systems. The positions of the maxima (centers of gravity) of the peaks $z_m =$ 0.45, 0.75, (0.90), 1.04, (1.19), 1.29, (1.45), 1.64, and 1.83 are in agreement (within an accuracy of ± 0.04) with those determined in Sect. 2. The exception consists only for peaks, represented in brackets, which are absent in the z-distribution for Mg II systems shown in Fig. 3. These peaks may appear due to statistical fluctuations, which become more noticeable in the case of shortage of the statistical material. Let us notice, however, that the existence of the peak at $z_m = 1.45$ is quite probable, since it shows up in the z-distribution of C IV at a significance level of 3σ.

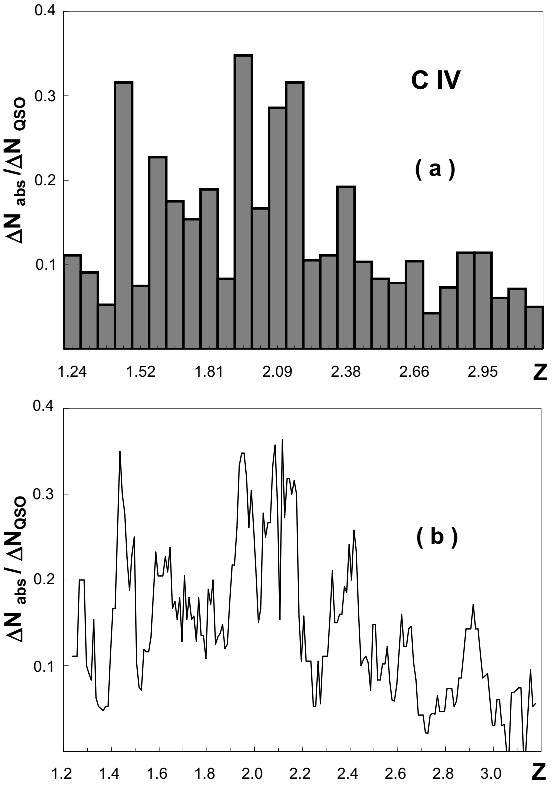

Fig. 9. Same as Fig. 2, but for the normalized distribution $\Delta N\text{abs}/\Delta N_{\text{QSO}}$.

Fig. 10 shows two normalized z-distributions of C IV and Mg II absorption systems in overlapping redshift range $z = 1.2 - 1.9$. The distributions are obtained using the sliding-average procedure with so–called line smoothing over each three neighboring points; the resulting bin size is $\Delta z = 0.071 + 0.01 + 0.01 = 0.091$. According to Eq. (9) 52 C IV and 20 Mg II absorption systems were sampled (5 common systems with the same

z_a). One can see that the positions of the peaks in the both distributions are in a good agreement. The correlation coefficient for these two distributions is $r = 0.323$, while for independent bins we would have $r_\beta = 0.250$ at dof= 60 and $\beta = 0.95$.

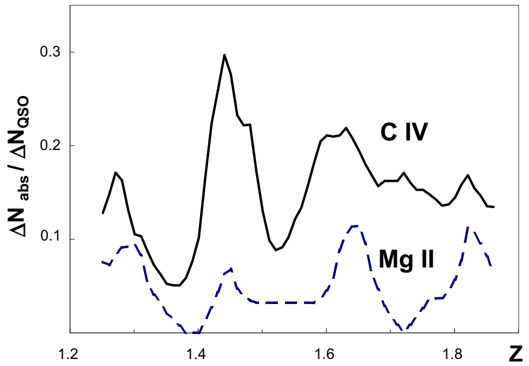

Fig. 10. Normalized distributions of C IV and Mg II absorption systems in the redshift range $z = 1.2 - 1.9$ (see text for details).

3.2. Isotropy of the normalized distributions

Fig. 11 shows the normalized two-dimensional distributions of C IV systems in the Equatorial and Galactic coordinates. The light and dark domains correspond to enhanced and reduced values of $\Delta N\text{abs}/\Delta N_{\text{QSO}}$, respectively. One can see an alternation of light and dark bands, similar to those in Fig. 7. There are a few continuous bands, in which the position of maxima of the z-distribution are independent of α_c within the errors (z_m = 1.45, 1.95, and 2.11). The other bands are more fragmented (z_m = 1.63, 1.78, 2.38, 2.63, and 2.91). The black domains in Fig. 11 correspond to those hemispheres (α_c, l_c) and redshift ranges, where ΔN_{QSO} and/or $\Delta N\text{abs}$ are not available. The increase of the number and the square of such "black" domains in Fig. 11, as compared to Fig. 7, is a result of an essential lack of statistical material. In the case of Mg II systems the two-dimensional distribution turns out to be still more uncertain than in Fig. 11. However, there are a few continuous bands (at $z_m = 0.45, 1.04, 1.29, 1.64$). The other can be treated as fragmentary.

Thus, our study of normalized distributions is free of selection effects but less statistically reliable. Nevertheless, it confirms the main results obtained in Sect. 2.3: *non-uniformity* in the z-distribution of the absorption-line systems and *independence* of the z-distribution on the direction of observation.

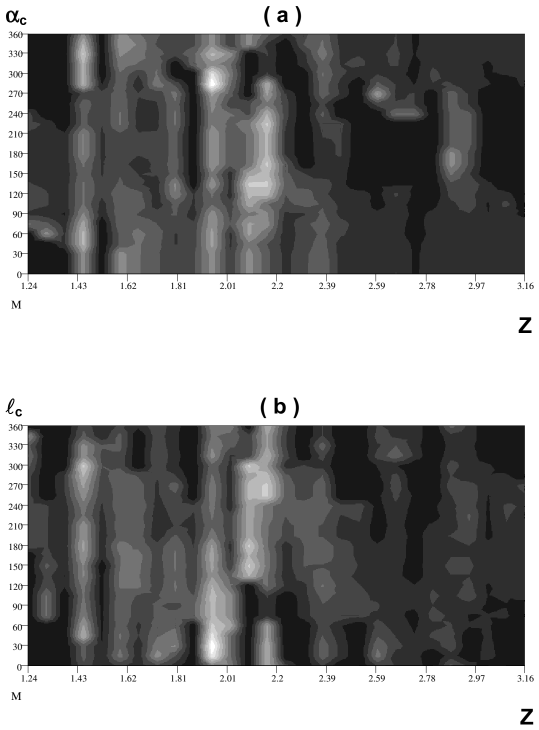

Fig. 11. Same as in Fig. 7 but for the normalized two-dimensional distributions of C IV systems.

4. Testing of clustering

It is worthwhile to test additionally a hypothesis that the set of maxima in the space-time distribution discussed here appears as a result of concentration of an essential part of absorbing matter towards clusters or superclusters of Galaxies (e.g., Quashnock et al. 1996). These regions of enhanced concentration of absorbers could be responsible for the peaks obtained, and might imitate, to some extent, the distribution of the peaks on the celestial sphere.

Some tests of the possible influence of clustering of matter are represented in Fig. 12a and b. Both figures show a sliding-average distribution of the C IV absorption-line systems based on the same statistics as used in Sect. 2.2 but with elimination of possible effects of the clustering. Fig. 12a shows the distribution of 261 out of 299 C IV absorption systems. Two sets of systems were omitted: (i) twofold and threefold associations of QSOs within $1^\circ \times 1^\circ$ square regions on the celestial sphere, (ii) five QSOs listed in Table 1 by Quashnock et al. (1996), displaying in their spectra ≥ 4 C IV absorbers within a $100h^{-1}$ Mpc interval ($h = H_0/(100\ \mathrm{km\ s^{-1}\ Mpc^{-1}})$, where H_0 is Hubble constant).

One can see that the positions of the peaks do not change after such a reduction of statistics. The correlation coefficient between the curves shown in Fig. 2b and Fig. 12a is high $r_{\mathrm{corr}} = 0.976$.

Fig. 12b shows the distribution of 136 out of 299 C IV absorption systems with elimination of all bunches of systems along different lines of sight with relative velocities less than 10 000km/s. One can see the same qualitative result as it is seen in Fig. 12a in spite of a strong reduction of statistics: the positions of the peaks do not change, although their outlines are essentially distorted. The correlation coefficient between the curves plotted in Fig. 2b and Fig. 12b is $r_{\mathrm{corr}} = 0.779$.

Thus, these tests may be regarded as arguments against the assumption that the set of peaks and depressions obtained is a result of clustering of absorption systems considered.

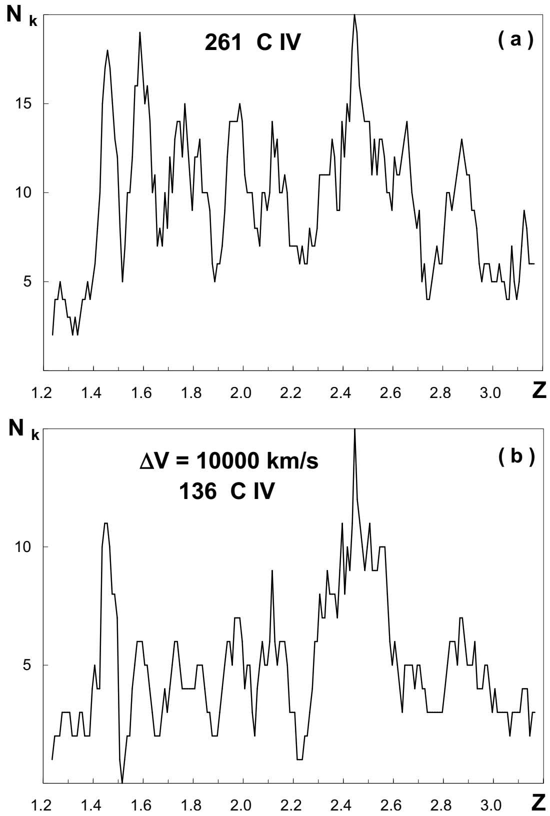

Fig. 12. Two tests for possible influence of clustering of absorbing matter. Same as Fig. 2b, but with elimination of two samples of C IV absorption systems: (a) groups of C IV absorbers indicated in Table 1 by Quashnock et al. (1996) as well as all associations of QSOs with their absorption systems within $1^\circ \times 1^\circ$ square regions on the sky. 261 C IV systems are left. (b) Groups of C IV absorbers along all lines of sight with relative velocities less than 10 000km/s. 136 C IV systems are left.

5. Testing of regularities

We tested possible regularity (periodicity) of the z-distribution obtained within the total interval $0.2 \leq z \leq 3.2$, exploring two independent methods: (1) regression analysis of the peak values z_m, and (2) power spectrum analysis of the available sample of redshifts. The search for periodicities was produced in respect of four trial functions on z:

$$\begin{aligned} f_a(z) &= \ln(1+z), \quad f_b(z) = (1+z)^{-1/2}, \\ f_c(z) &= (1+z)^{-1}, \quad f_d(z) = (1+z)^{-3/2}, \end{aligned} \tag{11}$$

corresponding to different cosmological models.

(1) The regression analysis of the common set of peaks obtained for the C IV and Mg II systems in Sect. 2.2 has been carried out to test for possible periodicities relative to the four trial functions of Eqs. (11). The results obtained for all functions turn out to have similar statistical uncertainties. However, a slightly lower dispersion of periodicity is found for the functions $f_a(z)$. In that case the regression equation is: $z_m + 1 = z_m(l) + 1 = \exp(a + \Delta_a\, l)$, where Δ_a is a shift of the function $\ln(1 + z_m)$ between two consecutive peaks $z_m(l+1)$ and $z_m(l)$, i.e., a period of peak positions, $l = 0, 1, 2, ..$ numerates the whole set of periods used in analysis, $m = 1, 2, ...$ numerates the whole set of the peaks z_m (in the general case $l + 1 \geq m$), a is starting constant. The results of this analysis, $\Delta_a = 0.065 \pm 0.002$ and $a = -0.014 \pm 0.022$, appear to be consistent with the hypothesis of periodicity of the sequence of values $\ln(1+z_m(l))$ corresponding to the set of maxima z_m obtained.

For comparison, let us represent the result of the regression analysis carried out for the function $f_b(z)$. We used the regression equation $z_m + 1 = z_m(l) + 1 = (b + \Delta_b\, l)^{-2}$, where Δ_b is a shift of the function $(1 + z_m)^{-1/2}$ between neighboring peaks $z_m(l + 1)$ and $z_m(l)$. In result we obtain $\Delta_b = 0.020 \pm 0.003$ and $b = 0.01 \pm 0.06$.

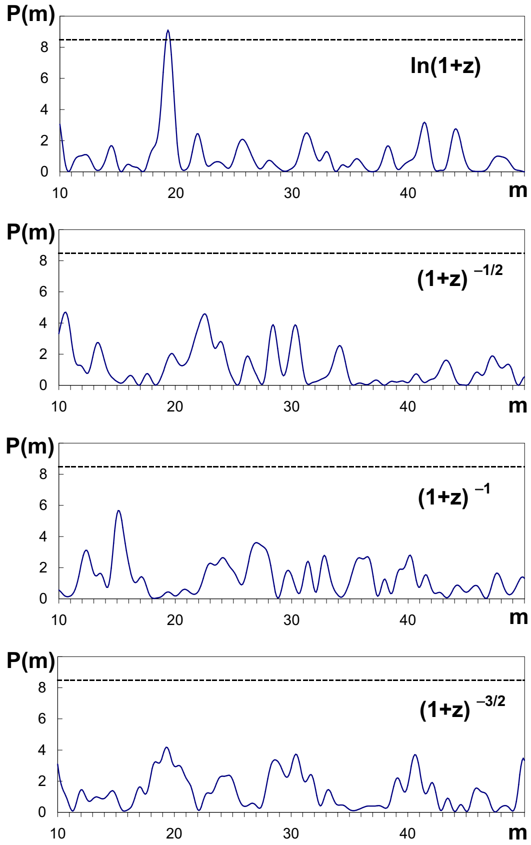

Fig. 13. Power spectra $P(m)$, m is number of harmonics, for the common z-distribution of C IV and Mg II systems ($z = 0.2 - 3.2$) obtained for four trial functions (see Eqs. (11)) indicated in each panel. Horizontal dashed lines denote confidence level $\beta = 0.950$.

(2) The power spectrum analysis was used to test periodicities with respect to the trial functions of Eqs. (11) for the sample of C IV and Mg II redshifts. This technique is independent of the procedures used in our previous analysis. The spectral power is defined in a standard way (see, e.g., Karlsson 1977, Arp et al. 1990):

$$\mathrm{P}(m) = \frac{1}{N}\left\{\left[\sum_{i=1}^{N}\cos\left(\frac{2\pi m f(z_i)}{F}\right)\right]^2 + \left[\sum_{i=1}^{N}\sin\left(\frac{2\pi m f(z_i)}{F}\right)\right]^2\right\}, \qquad (12)$$

where $N = 497$ is the number of redshift values used z_i $(i = 1, 2..N)$, $f(z_i) = f_a(z_i), ...f_d(z_i)$ are the trial functions given in Eq. (11), $F = f(z_N) - f(z_1)$ is the total interval of variations of $f(z_i)$, m is harmonic number. The existence of periodicity appears as a peak in the power spectrum $\mathcal{P} = \max\,(\mathrm{P}(m))$ with a confidence probability

$$\beta \geq [1 - \exp(-\mathcal{P})]^{N/2}\,, \qquad (13)$$

where $N/2$ is the maximum number of possible peaks (periodicities) in a z-distribution of N redshifts.

The results of this analysis for all trial functions given by Eqs. (11) are represented in Fig. 13. One can see that in the interval of m considered the only significant peak $\mathrm{P}(m)$ appears for the function $f(z) = f_a(z)$ at $m = 19$ on the confidence level $\beta = 0.973$ ($> 2\sigma$). This peak corresponds to a periodicity of the distribution in respect to the function $\ln(1+z)$ with a period $\tilde{\Delta}_a = F/m = 0.066 \pm 0.003$. This is quite consistent with the result of the regression analysis given above.

Let us note that the power spectrum analysis does not depend on the choice of redshift bin and may be treated as additional evidence for the existence of the peak-depression structure for the redshifts distribution discussed in Sect. 2.2.

6. Discussion and conclusions

The statistical analysis of the distributions of C IV and Mg II absorption-line systems with redshifts $z = 0.2 - 3.2$ leads to the following conclusions.

(1) The distributions of the absorption systems are not uniform (at the confidence level $\beta > 0.998$), and have alternating maxima and minima. The maxima in the distribution of C IV systems correspond to $z_m = 1.46$, 1.60, 1.78, 1.98, 2.14, 2.45, 2.64, and 2.86 (± 0.04). The maxima in the distribution of Mg II systems appear at $z_m = 0.44$, 0.77, 1.04, 1.30, 1.66, and 1.78 (± 0.04). Most of these peaks have a significance $> 2\sigma$, however, some of them are less significant, most likely due to lack of statistics.

(2) Values of z_m corresponding to the maxima of the z-distributions were found to be independent (within statistical uncertainties) of hemisphere orientations. In particular, there is a correlation of the z-distributions in pairs of opposite (independent) hemispheres on a significance level $\gtrsim 2\sigma$. This is evidence of statistical isotropy of the distributions.

(3) The distribution obtained can be imagined as a series of embedded spheres of absorbing material (onion-like structure) corresponding to the

peaks at z_m indicated above. Such structure may be considered as a Global Large-Scale Structure (GLSS) of the space-time distribution, and most likely is associated with an appearance of pronounced and depressed epochs in the course of cosmological evolution.

(4) The characteristic time interval T between the maxima of pronounced epochs strongly depends on the cosmological model and on a trial function used (see Sect. 5). For instance, one can estimate that $T_a = \Delta_a/H_0 = (650 \pm 30)h^{-1}$ Myr for the trial function $f_a(z)$ from Eq. (11), and $T_b = 2\Delta_b/H_0 = (400 \pm 60)h^{-1}$ Myr for the trial function $f_b(z)$.

Let us stress that there is no contradiction between the GLLS considered and the statement that all points of space are equivalent. The GLLS does not correspond to a fixed cosmic time, but displays the time evolution. As an example of the pronounced epochs appearing as isotropic elements of the GLSS one may considered the epoch of the hydrogen recombination associated with formation of the Cosmic Microwave Background.

The appearance of the pronounced epochs may be understood by taking into account some intrinsic evolutionary properties of galaxies and clusters. On the other hand, it can be understood in the framework of cosmological scenarios taking into account a scalar field or phase transitions in the late stages of the evolution. It can lead to quasi-periodic oscillations of the effective gravitational constant G, and/or the Hubble constant H, and/or the cosmological constant Λ_0 (see, for example, Morikawa 1991 , Damour & Polyakov 1994, Sisterna & Vucetich 1994).

Our results do not exclude the existence of the spatial structures – LSS (see, e.g., Einasto et al. 1997). It should be note only, that the bin width adopted in our paper is appreciably larger than the values Δz associated with peculiar motions of galaxies, including their flows in the clusters and superclusters, as well as possible gravitational shifts. Hence, the non-uniformity of the distributions of absorbing material due to spatial structures seems to be averaged out in the present consideration.

Let us note that a set of peaks in the z-distribution of quasars was found by Burbidge & Burbidge (1967) and confirmed later by many authors (see, e.g., Arp et al. 1990). Some of the maxima in the distributions of absorption material were also reported earlier (e.g.,Chu & Zhu 1989, Arp et al. 1990). For instance, for a sample of QSO absorption-line systems within the so called 12^h region ($8^h < \alpha < 17^h$; $-01^\circ < \delta < 42^\circ$) Arp et al. (1990) found three conspicuous peaks at $z_m = 1.47, 1.97, 2.85$ in the distribution of C IV and Mg II absorption systems. One can note that these three peaks are consistent within statistical uncertainties with corresponding peaks found in our analysis.

Recently, Liu & Hu (1998) have shown a quite significant set of alternating peaks and depressions in the dependence of the photons mean free path $\lambda_0(z)$ on the redshift z. They found that fitting function for the quantity $\lambda_0(z)$ comprises a periodic dependence on the time variable $t = t_0(1+z)^{-3/2}$ with a period $T = 155\ h^{-1}$ Myr. It yields positions of noticeable minima of $\lambda_0(z)$, which turn out to be equal to $z_{\rm min} = 1.79,\ 2.02,\ 2.30,\ 2.66,\ 3.13$. The minima of $\lambda_0(z)$ approximately correspond to the maxima of the number density of the absorption redshifts discussed in our paper. Comparing this set of $z_{\rm min}$ with the values of z_m obtained in our study one can see some qualitative agreement of the both sets of the values. Moreover, the regression analysis described in Sect. 5 yields the same period $T_d = 2\Delta_d/(3H_0) = (150 \pm 50)h^{-1}$ Myr but with lower statistical significance than the periods T_a and T_b represented above.

The periodicity in the positions of the QSO peaks relative to the function $\ln(1+z)$ was first pointed out by Karlsson (1971), (1977). It was found that shifts between consecutive peaks correspond to the period $\Delta_a \approx 0.20$. This period was confirmed by many authors (see, e.g., Fang et al. 1982, Chu & Zhu 1989, Arp et al. 1990, Karlsson 1990) on more extensive statistical material. In Sect. 5 we found a periodicity of the redshifts relative to the same function, but the period obtained ($\Delta_a = 0.065 \pm 0.002$) differs from that mentioned above exactly by a factor 3 (within the statistical uncertainties).

Characteristic distances between the maxima in the distribution of absorbing material can be also estimated in a comoving reference frame. For instance, using the quantity of comoving distance $r_z = 2c/H_0[1-(1+z)^{-1/2}]$ at $q = 1/2$ and $\Omega = 1$, where q and Ω are standard cosmological parameters, and the results of the regression analysis represented in Sect. 5 for function $f_b(z)$, one obtains $2c\Delta_b/H_0 = (120 \pm 20)h^{-1}$ Mpc. This scale of inhomogeneities coincides, within the errors, with the values $128h^{-1}$ Mpc obtained by Broadhurst et al. (1990) for $z \leq 0.5$, with $100h^{-1}$ Mpc obtained by

Landy et al. (1996) for $z \leq 0.2$, and with $120h^{-1}$ Mpc obtained by Einasto et al. (1997) for $z \leq 0.12$.

Let us note finally, that at small values of z the velocities of the peculiar motions of galaxies are comparable with the velocities of the cosmological expansion. Therefore, we expect that, if sufficient statistical material is collected, the GLSS should be more pronounced at higher redshifts.

Acknowledgements. The authors acknowledge helpful discussions with the referee. This work was supported by RFBR (Grant No. 99–02–18232), and by "Cosmion" (Center for Cosmoparticle Physics).

References

Arp H., Bi H.G., Chu Y., Zhu X., 1990, A&A 239, 33
Bahcall N.A., 1995, in Böhringer H., Morfill G.E., Trümper J.E. (eds.) 17th Texas Symposium on Relativistic Astrophysics and Cosmology. NY 636
Bergeron J., D'Odorico S., Kunth D., 1987, A&A 180, 1
Boisse P., Bergeron J., 1985, A&A 145, 59
Broadhurst T.J., Ellis R.S., Koo D.C., Szalay A.S., 1990, Nature 343, 726
Burbidge G.R., Burbidge E.M., 1967, ApJ 148, L107
Caulet A., 1989, ApJ 340, 90
Chu Y., Zhu X., 1989, A&A 222, 1
Damour T., Polyakov A.M., 1994, Nucl.Phys. B423, 532
Einasto J., Einasto M., Gottlöber S., et al., 1997, Nature 385, 139
Fang L., Chu Y., Liu Y., Cao Ch., 1982, A&A 106, 287
Foltz C.B., Weymann R.J., Peterson B.M., et al., 1986, ApJ 307, 504
Junkkarinen V., Hewitt A., Burbidge G., 1991, ApJS 77, 203
Karlsson K.G., 1971, A&A 13, 333
Karlsson K.G., 1977, A&A 58, 237
Karlsson K.G., 1990, A&A 239, 50
Khare P., York D.G., Green R., 1989, ApJ 347, 627
Landy S.D., Shectman S.A., Lin H., Kirshner R.P., Oemler A.A., Tucker D., 1996, ApJ 456, L1
Lanzetta K.M., Bowen D.V., 1992, ApJ 391, 48
Lanzetta K.M., Turnshek D.A., Wolfe A.M., 1987, ApJ 322, 739
Liu Y., Hu F., 1998, A&A 329, 821
Morikawa M., 1991, ApJ 369, 20
Peebles P.J.E., 1993, Principles of Physical Cosmology, Princeton Univ., Princeton.
Petitjean P., Bergeron J., 1990, A&A 231, 309
Quashnock J.M., Vanden Berk D.E., York D.G., 1996, ApJ 472 , L69
Robertson J.G., Shaver P.A., Surdej J., Swings J.P., 1986, MNRAS 219, 403
Robertson J.G., Morton D.C., Blades J.C., York D.G., Meyer D.M., 1988, ApJ 325, 635
Ryabinkov A.I., Varshalovich D.A., Kaminker A.D., 1998, Astron. Lett. 24, 418
Sargent W.L.W., Steidel C.C., 1987, ApJ 322, 142
Sargent W.L.W., Young P., Boksenberg A., 1982, ApJ 252, 54
Sargent W.L.W., Boksenberg A., Steidel C.C., 1988a, ApJS 68, 539
Sargent W.L.W., Steidel C.C., Boksenberg A., 1988b, ApJ 334, 22
Sargent W.L.W., Steidel C.C., Boksenberg A., 1989, ApJS 69, 703
Sargent W.L.W., Steidel C.C., Boksenberg A., 1990, ApJ 351, 364
Sisterna P.D., Vucetich H., 1994, Phys.Rev.Lett. 72, 454
Steidel C.C., 1990, ApJS 72, 1
Steidel C.C., Sargent W.L.W., 1992, ApJS 80, 1
Turnshek, D.A., Wolfe A.M., Lanzetta K.M., et al., 1989, ApJ 344, 567
Val'tts I.E., 1991, AZh 68, 261
Wolfe A.M., Turnshek D.A., Smith H.E., Cohen R.D., 1986, ApJS 61, 249
Young P., Sargent W.L.W., Boksenberg A., 1982, ApJ 252, 10